

Benzyl Isothiocyanate (BITC) Induces G₂/M Phase Arrest and Apoptosis in Human Melanoma A375.S2 Cells through Reactive Oxygen Species (ROS) and both Mitochondria-Dependent and Death Receptor-Mediated Multiple Signaling Pathways

Su-Hua Huang,[†] Liu-Wei Wu,[†] An-Cheng Huang,[‡] Chien-Chih Yu,[§] Jin-Cherng Lien,[#] Yi-Ping Huang,[⊥] Jai-Sing Yang,[▲] Jen-Hung Yang,[△] Yu-Ping Hsiao,^{●,○} W. Gibson Wood,[▼] Chun-Shu Yu,^{*,§,||} and Jing-Gung Chung^{*,†,⊗,||}

[†]Department of Biotechnology, Asia University, Taichung 413, Taiwan

[‡]Department of Nursing, St. Mary's Medicine Nursing and Management College, Yilan 266, Taiwan

[§]School of Pharmacy, China Medical University, Taichung 404, Taiwan

[#]Graduate Institute of Pharmaceutical Chemistry, China Medical University, Taichung 404, Taiwan

[⊥]Department of Physiology, China Medical University, Taichung 404, Taiwan

[▲]Department of Pharmacology, China Medical University, Taichung 404, Taiwan

[△]School of Medicine, Tzu Chi University, and Department of Dermatology, Buddhist Tzu Chi General Hospital, Hualien 970, Taiwan

[●]Institute of Medicine, School of Medicine, Chung Shan Medical University, Taichung 402, Taiwan

[○]Department of Dermatology, Chung Shan Medical University Hospital, Taichung 402, Taiwan

[▼]Department of Pharmacology, University of Minnesota, School of Medicine, Geriatric Research, Education and Clinical Center, VA Medical Center, Minneapolis, Minnesota 55455, United States

[⊗]Department of Biological Science and Technology, China Medical University, Taichung 404, Taiwan

ABSTRACT: Benzyl isothiocyanates (BITC), a member of the isothiocyanate (ITC) family, inhibits cell growth and induces apoptosis in many types of human cancer cell lines. The present study investigated mechanisms underlying BITC-induced apoptosis in A375.S2 human melanoma cancer cells. To observe cell morphological changes and viability, flow cytometric assays, cell counting, and a contrast-phase microscopic examination were carried out in A375.S2 cells after BITC treatment. Cell cycle distribution and apoptosis were assessed with the analysis of cell cycle by flow cytometric assays, DAPI staining, propidium iodide (PI), and annexin V staining. Apoptosis-associated factors such as reactive oxygen species (ROS) formation, loss of mitochondrial membrane potential ($\Delta\Psi_m$), intracellular Ca²⁺ release, and caspase-3 activity were evaluated by flow cytometric assays. Abundance of cell cycle and apoptosis associated proteins was determined by Western blotting. AIF and Endo G expression was examined by confocal laser microscope. Results indicated that (1) BITC significantly reduced cell number and induced cell morphological changes in a dose-dependent manner in A375.S2 cells; (2) BITC induced arrest in cell cycle progression at G₂/M phase through cyclin A, CDK1, CDC25C/Wee1-mediated pathways; (3) BITC induced apoptosis and increased sub-G₁ population; and (4) BITC promoted the production of ROS and Ca²⁺ and loss of $\Delta\Psi_m$ and caspase-3 activity. Furthermore, BITC induced the down-regulation of Bcl-2 expression and induced up-regulation of Bax in A375.S2 cells. Moreover, BITC-induced cell death was decreased after pretreatment with *N*-acetyl-L-cysteine (NAC, a ROS scavenger) in A375.S2 cells. In conclusion, the results showed that BITC promoted the induction of G₂/M phase arrest and apoptosis in A375.S2 human melanoma cells through ER stress- and mitochondria-dependent and death receptor-mediated multiple signaling pathways. These data suggest that BITC has potential as an agent for the treatment of melanoma.

KEYWORDS: BITC, apoptosis, ROS, G₂/M phase arrest, mitochondria, A375.S2 melanoma cells

■ INTRODUCTION

Apoptosis plays an important role in normal homeostasis and is involved in multiple steps leading to cell death. Two major pathways described as the extrinsic (death receptor) pathway and the intrinsic (mitochondrial) pathway mediate apoptosis.¹ The extrinsic cell death pathway is involved in Fas ligand (FasL) binding to Fas receptors that induces intracellular signaling and the cleavage and activation of caspase-8.^{2,3} Caspase-8 can

then cleave effector caspase-3 to induce apoptosis directly.⁴ The intrinsic cell death pathway is involved in cleavage of Bid (a pro-apoptotic protein) and changes the ratio of Bax/Bcl-2, causing

Received: August 1, 2011

Revised: December 9, 2011

Accepted: December 12, 2011

Published: December 12, 2011

mitochondria dysfunction (loss of mitochondrial membrane integrity)⁵ and the release of cytochrome *c*.⁶ Cytochrome *c* activates caspase-9 and subsequently leads to the activation of effector caspase-3, resulting in apoptosis.^{6,7}

It is well documented that phytochemicals found in certain food substances protect against cancer. Cruciferous vegetables are recognized as potential diet components that may decrease the risk of developing various types of malignancies.^{8–10} Isothiocyanates (ITCs), one kind of phytochemical, are major components in cruciferous vegetables, which play significant and important roles in anticarcinogenic effects in animal models.¹¹ The inhibition of phase I enzymes (cytochrome P-450s), which are involved in the activation of carcinogens and/or induction of phase II detoxifying enzymes (glutathione S-transferases, quinone reductase, and UDP-glucuronosyltransferases) is the major cancer chemopreventive activity of ITCs.¹²

Benzyl ITC (BITC), one of the ITCs, has been shown to induce apoptotic cell death in several different human cancer cell types such as breast cancer cells,^{13,14} bladder cancer cells,¹⁵ prostate cancer cells,¹⁶ ovarian cancer cells,^{17,18} and leukemia cells.^{19,20} Recently, we also found that BITC-mediated generation of reactive oxygen species (ROS) causes cell cycle arrest and induces apoptosis via activation of caspase-3, mitochondria dysfunction, and nitric oxide in human osteogenic sarcoma U-2 OS cells.²¹ It was also reported that antioxidant function contributed to BITC-mediated chemoprevention and superoxide generation against inflammation-related carcinogenesis in inflammatory leukocytes.²²

Although BITC acts as an anticancer agent via the inhibition of cell growth, little is known about the anticancer effect of BITC on human melanoma A375.S2 cells. Therefore, in the present study, we evaluated the effects of BITC on cell growth and death in A375.S2 cancer cells. We found that BITC-induced cell death is mediated through G₂/M phase arrest and ROS, caspases, and modification of mitochondrial function in A375.S2 cells.

MATERIALS AND METHODS

Chemicals and Reagents. BITC, dimethyl sulfoxide (DMSO), propidium iodide (PI), RNase A, and Triton X-100 were obtained from Sigma-Aldrich Corp. (St. Louis, MO). In Western blot assay, the primary and secondary antibodies were purchased from Santa Cruz Biotechnology Inc. (Santa Cruz, CA). Minimum essential medium (MEM), Dulbecco's modified Eagle's medium (DMEM), fetal bovine serum (FBS), penicillin/streptomycin, L-glutamine, and the fluorescent probes 4',6-diamidino-2-phenylindole (DAPI), 2,7-dichlorodihydrofluorescein diacetate (H₂DCF-DA), Fluo-3/AM, 3'-dihexyloxycarbocyanine iodide (DiOC₆), DAF-FM diacetate, and 10-nonyl acridine orange (NAO) were purchased from Invitrogen Life Technologies (Carlsbad, CA).

Cell Culture. The human melanoma cell line (A375.S2) was obtained from the Food Industry Research and Development Institute (Hsinchu, Taiwan) and maintained in MEM.²³ The human keratinocyte cell line (HaCaT) was kindly provided by Dr. Jen-Hung Yang (Department of Dermatology, Buddhist Tzu Chi General Hospital) and seeded in DMEM.²⁴ All media were supplemented with 10% FBS, 1% antibiotics (100 units/mL penicillin, and 100 µg/mL streptomycin), and 2 mM L-glutamine under incubation and humidified 5% CO₂ and 95% air at 1 atm and at 37 °C. The cells were examined each day, and the medium was changed every 2 days.

Determinations of Cell Viability and Morphology in A375.S2 and HaCaT Cells after Exposure to BITC. Both cell lines at an initial density of 2 × 10⁵ cells/mL were incubated with 5, 10, and 20 µM BITC and an equal amount of DMSO for control cells for 24 and 48 h at 37 °C. At the end of treatment, A375.S2 cells were examined and photographed under a phase-contrast microscope at 200× magnification to determine morphological changes. Cells were

then harvested for the determination of viability using a FACSCalibur flow cytometer (Becton-Dickinson, Franklin Lakes, NJ) as previously described.²³

Determinations of Cell Cycle Distribution in A375.S2 Cells after Treatment with BITC. Cells were seeded at an initial density of 2 × 10⁵ cells/mL and incubated with 10 µM BITC or vehicle (DMSO, 1% in culture media) for 0, 24, 36, and 48 h. After incubation, the cells were trypsinized, washed with PBS, and fixed with 70% ethanol overnight at -20 °C. Cells were then washed twice with cold PBS containing 1% bovine serum albumin (BSA) and stained with PI working solution (100 µg/mL RNase A and 40 µg/mL PI and 0.1% Triton X-100) at room temperature for 1 h in the dark. DNA content analysis was accomplished using a flow cytometric method, and data were analyzed with a ModFit program as previously described.²⁵ Fractions of cells in G₀/G₁, S, and G₂/M phases and sub-G₁ (apoptosis) were measured as described elsewhere.^{26,27}

Assessments of Apoptosis by Flow Cytometric Assay and DNA Gel Electrophoresis in A375.S2 Cells after BITC Treatment. Cell apoptosis was determined using the annexin V-FITC/PI apoptosis detection kit (BD Pharmingen, San Diego, CA) and DNA gel electrophoresis. Cells were plated at a density of 2 × 10⁵ cells/mL and incubated with 0, 5, 10, and 20 µM BITC or vehicle (DMSO, 1% in culture media) for 24 h. At the end of the incubation, cells were harvested, and the percentage of apoptotic cells by flow cytometry was assayed as previously described.²⁸ Cells were harvested and DNA isolated by using a DNA isolation kit (Genemark Technology Co., Ltd. Tainan, Taiwan). DNA gel electrophoresis was used to determine the extent of DNA fragmentation as previously described.²⁵ Apoptosis was also examined using DAPI staining. Cells at a density of 1 × 10⁵ cells/mL in 6-well plates were incubated with 0, 5, 10, 15, and 20 µM BITC or vehicle (DMSO, 1% in culture media) for 24 h. At the end of the incubation, cells were stained with DAPI and photographed using a fluorescence microscope as described elsewhere.^{29,30}

Effects of BITC on DNA Damage in A375.S2 Cells Using the Comet Assay. Cells were plated at a density of 5 × 10⁵ cells/mL and incubated with 0, 5, 10, 15, and 20 µM BITC or vehicle (DMSO, 1% in culture media) for 24 h. At the end of the incubation period, cells were harvested, and DNA damage was determined using the comet assay and analyzed using CometScore software (Tritek Corp, Sumerduck, VA) as previously described.^{25,31}

Determination of ROS, Mitochondrial Membrane Potential (ΔΨ_m), Intracellular Ca²⁺ and NO Release, and Levels of Cardiolipin Oxidation and Caspase-3 Activity in A375.S2 Cells by Flow Cytometry after Exposure to BITC. Cells at an initial density of 2 × 10⁵ cells/mL in 12-well plates were incubated with 10 µM BITC or vehicle (DMSO, 1% in culture media) for 0.5, 1, 2, 3, 6, 12, 24, 36, or 48 h to detect if this compound would affect ROS, ΔΨ_m, Ca²⁺, NO, and caspase-3 that were measured as previously described.^{21,25} Cells were harvested and washed with PBS twice, resuspended in 500 µL of H₂DCF-DA (10 µM) for ROS, DiOC₆ (1 µmol/L) for ΔΨ_m, Fluo-3/AM (2.5 µg/mL) for Ca²⁺ release, and DAF-FM (5 µM) for monitoring NO and NAO (500 nM) for cardiolipin oxidation. Cells were incubated at 37 °C for 30 min and then were analyzed for the levels of ROS, ΔΨ_m, Ca²⁺, NO, and cardiolipin oxidation by flow cytometry as previously described.^{21,25} Caspase-3 activity was determined using caspase-3 substrate (PhiPhiLux-G₁D₂ kit, OncoImmunin, Inc., Gaithersburg, MD) flow cytometry as described elsewhere.²⁵

Western Blot Analysis for Protein Levels in A375.S2 Cells after Exposure to BITC. Cells in 6-well plates at a density of 1 × 10⁶ cells/well were treated with 10 µM BITC, or DMSO solvent, for 0, 12, 24, 36, and 48 h. At the end of each incubation, cells were harvested and washed twice with cold PBS, then scraped and washed twice, and then centrifuged at 1000g for 5 min at 4 °C. Cell protein was extracted into a high-salt buffer (PRO-PREP protein extraction solution, iNtRON Biotechnology, Seongnam, Gyeonggi-Do, Korea), and protein concentrations were determined by a BCA Protein Assay kit (Pierce, Rockford, IL). Sodium dodecyl sulfate-polyacrylamide gel electrophoresis (SDS-PAGE) was used to separate proteins as previously described.^{16,21,23} Protein samples (30 µg) were loaded on a 12% gel SDS-PAGE and subjected to electrophoresis. Samples were

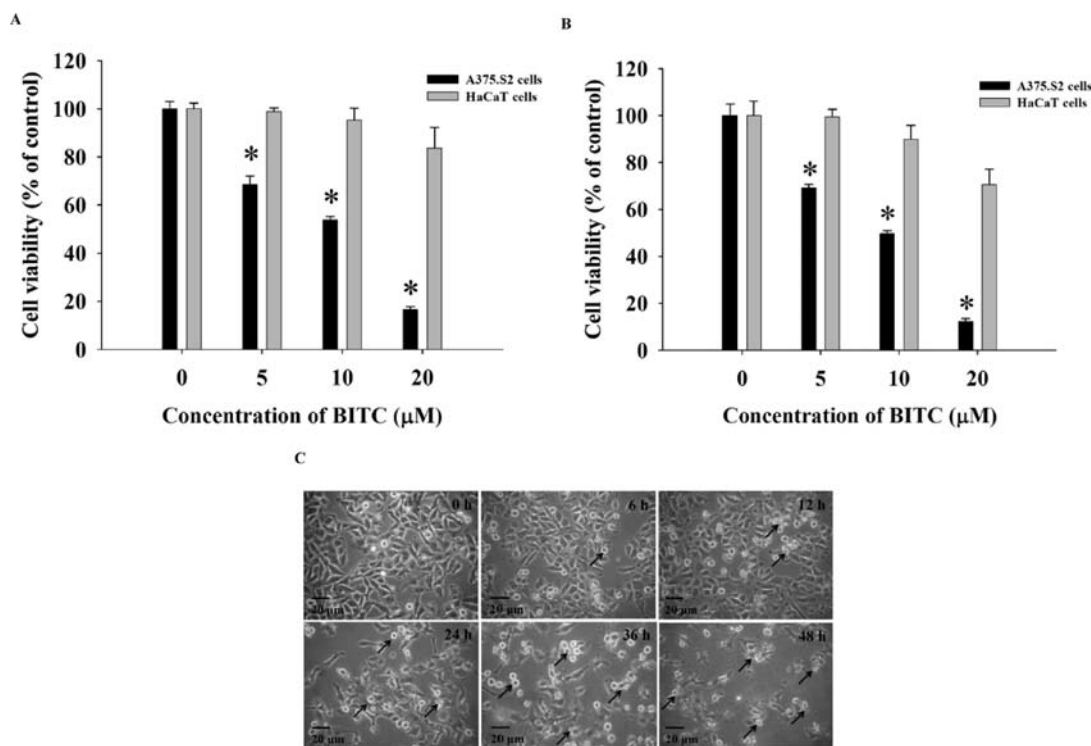


Figure 1. BITC decreased the percentage of viability and induced cell morphological changes in human melanoma A375.S2 cells in vitro. A375.S2 cells or human normal HaCaT cells at a density of 2×10^5 cells/well in 12-well plates were treated with 0, 5, 10, and 20 μM BITC and then harvested for the determination of percentage of viable cells for 24 h (A) and 48 h (B) of exposure. Cell morphology was examined, and then cells were photographed by a phase-contrast microscope (C) as described under Materials and Methods. The arrows show the shrinkage and rounding of apoptotic cells. Data are presented as the mean \pm SD in triplicate. $p < 0.05$ is significantly different compared between BITC- and DMSO-treated groups.

then transferred to Immobilon-P transfer membrane (Millipore, Bedford, MA) and individually incubated with the appropriate primary antibodies (Santa Cruz Biotechnology Inc.) followed by secondary antibodies. The antibody–protein complexes were detected using ECL kit (Immobilon Western HRP substrate, Millipore) and autoradiography using X-ray film according to the manufacturer's instructions.^{23,29}

Co-localization of Proteins in A375.S2 Cells Treated with BITC. Cells were plated on 4-well chamber slides at a density 5×10^4 cells/well and treated with 10 μM BITC for 12 h. Cells were then fixed in 3% formaldehyde (Sigma-Aldrich Corp.) in PBS for 15 min followed by permeabilization with 0.1% Triton X-100 in PBS for 1 h with blocking of nonspecific binding sites using 2% BSA.²⁶ The fixed cells were stained by using primary antibody anti-AIF and -Endo G (1:100) overnight. Cells were then washed three times with PBS and incubated with secondary antibody (FITC-conjugated goat anti-mouse IgG at 1:100 dilution) (green fluorescence). Cells were washed twice with PBS and stained with PI (red fluorescence) for nuclei. Photomicrographs were obtained using a Leica TCS SP2 confocal spectral microscope as previously described.^{25,29}

Statistical Analysis. Values are expressed as the mean \pm SD, and statistical analysis was calculated by Student's *t* test; a *p* value of <0.05 was considered to be statistically significant. All experiments were performed in triplicate.

RESULTS

BITC Altered Cell Morphology and Reduced the Percentage of Viable A375.S2 Cells. The results from the flow cytometric assay are shown in Figure 1A,B, which indicated that the percentage of viable cells was decreased when the concentration of BITC was increased for 24 h (Figure 1A) and 48 h (Figure 1B) exposure, and these effects were a dose- and time-dependent response. The half-maximal inhibitory

concentration (IC_{50}) of BITC was 9.76 μM after a 48 h treatment. It is reported that HaCaT cells are a nontumorigenic phenotype^{24,32} and have been used as a model for skin toxicity studies in in vitro model.^{33,34} Importantly, we found that BITC had less cytotoxic effect on normal human keratinocyte HaCaT cells when compared to A375.S2 melanoma cells. Moreover, BITC at the 10 μM concentration induced morphological changes in a time-dependent manner as seen in Figure 1C.

BITC Affected Cell Cycle Distribution and Triggered Apoptosis in A375.S2 Cells. To investigate the mechanisms leading to loss of cells induced by BITC, we tested whether the compound stimulates cell cycle arrest and apoptosis. The DNA content of cells was measured by flow cytometry. As shown in Figure 2A, treatment of A375.S2 cells with 10 μM BITC increased the percentage of cells in G_2/M phase (G_2/M phase arrest) after 24, 36, and 48 h of exposure (Figure 2A), but decreased the percentage of cells in G_0/G_1 and S phases. BITC caused an increase of the G_2/M phase fraction from 12 to 50%, as compared to control samples (Figure 2B).

BITC Induced Apoptosis, DNA Damage, Chromatin Condensation, and DNA Fragmentation in A375.S2 Cells. To evaluate BITC-induced apoptosis, DNA damage, chromatin condensation, and DNA fragmentation, cells were treated with 10 μM BITC for indicated intervals of time or with various concentrations of BITC for 24 h. Cells were isolated for flow cytometry by using an annexin V-FITC/PI kit, DAPI staining, comet assay, and DNA gel electrophoresis assays. The results are shown in Figure 3A–D, which indicated that the percentage of annexin V binding A375.S2 cells significantly increased in a time-dependent manner after treatment for 6–24 h

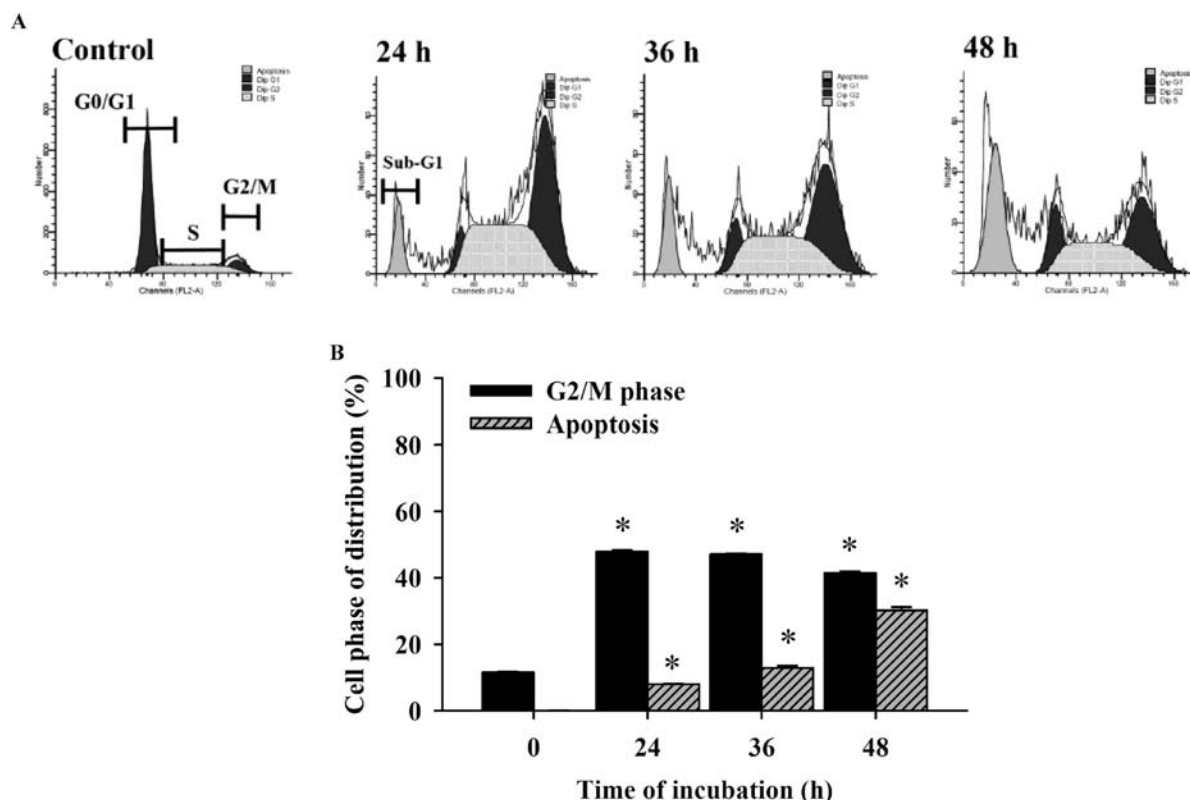


Figure 2. BITC caused G₂/M phase arrest in A375.S2 cells: (A) representative profiles of DNA content; (B) percentage of cells in G₀/G₁, S, and G₂/M phases in A375.S2 cells. Cells at a density of 2×10^5 cells/well were placed in 12-well plates and then were treated without and with 10 μ M BITC for 24, 36, and 48 h. Cells were harvested for evaluating the cell cycle distribution by flow cytometric assay as described under Materials and Methods. Data are revealed as a representative experiment in triplicate with similar results.

(8.2–25.51%, $p < 0.05$) (Figure 3A). BITC induced DNA condensation as shown by an increase in fluorescence intensity (Figure 3B), DNA damage as seen by increased comet tail (Figure 3C,D), and an increased DNA ladder (apoptosis-related DNA laddering) (Figure 3E). The higher dose of BITC showed the longest comet tail (Figure 3C) and heavy white color on nuclei, but there was a low number of cells (Figure 3B) but with high fluorescence intensity. These results indicate that BITC produces DNA damage and chromatin condensation in A375.S2 cells.

BITC Affected ROS Production, Mitochondrial Membrane Potential ($\Delta\Psi_m$), Intracellular Ca^{2+} Release, NO Production, Cardiolipin Oxidation (NAO), and Caspase-3 Activity in A375.S2 Cells. For investigating the roles of ROS, $\Delta\Psi_m$, Ca^{2+} , NO, NAO, and caspase-3 activity on BITC-induced DNA damage, fragmentation, and apoptosis in A375.S2 cells, cells were treated with 10 μ M BITC for various time periods. The results shown in Figure 4 indicated that BITC increased ROS levels (Figure 4A), Ca^{2+} (Figure 4C), NO (Figure 4D), and caspase-3 activity (Figure 4E), but it decreased levels of $\Delta\Psi_m$ (Figure 4B) and NAO (Figure 4E) in A375.S2 cells. These effects occurred in a time-dependent manner.

BITC Altered G₂/M Arrest and Apoptosis-Associated Proteins in A375.S2 Cells. To investigate the molecular mechanisms of BITC-induced G₂/M phase arrest and apoptosis in A375.S2 cells, we determined the G₂/M phase-modulated relative and apoptotic protein levels. Results shown in Figure 5A indicate that the levels of cyclin A, CDK1, and CDC25C were decreased, but the levels of Chk1 and Wee1 were increased. These protein changes were associated with BITC-induced G₂/M phase arrest in A375.S2 cells. On the basis of

these results, we suggest that BITC-induced G₂/M phase arrest in A375.S2 cells involves CDC25C/cyclinA/Wee1 signaling. Apoptosis-associated protein levels and results are shown in Figure 5B–D, which indicated that BITC promoted the levels of Bax (Figure 5B), cytochrome *c*, Apaf-1, caspase-9 and -3, AIF, and Endo G (Figure 5C), and Fas, FasL, FADD, and caspase-8 (Figure 5D), but reduced levels of Bcl-2 and Bid (Figure 5B) that could contribute to cell apoptosis. On the basis of these results, we propose that BITC-triggered apoptosis is carried out through mitochondria-, Fas-, and caspase-3-dependent pathways. Furthermore, results from Figure 5E,F indicate that BITC increased the levels of GADD153 and GRP78 (Figure 5E), which are hallmarks of ER stress. Results from Figure 5F indicated that BITC promoted the levels of catalase, SOD (Mn), and SOD (Cu/Zn). Taken together, these findings indicate that BITC-induced apoptotic cell death in A375.S2 cells occurs via ER stress and intrinsic and extrinsic multiple signaling pathways.

BITC Stimulated AIF and Endo G Translocation to Nuclei in A375.S2 Cells. To confirm BITC acting on AIF and Endo trafficking, we examined the levels of AIF and Endo G by immune staining and confocal microscopy. The results are shown in Figure 6, which indicated that BITC promoted protein trafficking of AIF and Endo G to the nucleus in A375.S2 cells. These results indicated that BITC-induced apoptosis occurs via mitochondria-dependent and caspase-independent pathways in A375.S2 cells.

BITC Altered Viable Cell Number, Morphology, DAPI Staining, ROS Production, and $\Delta\Psi_m$ Level in A375.S2 Cells after Pretreatment with NAC. To further examine the

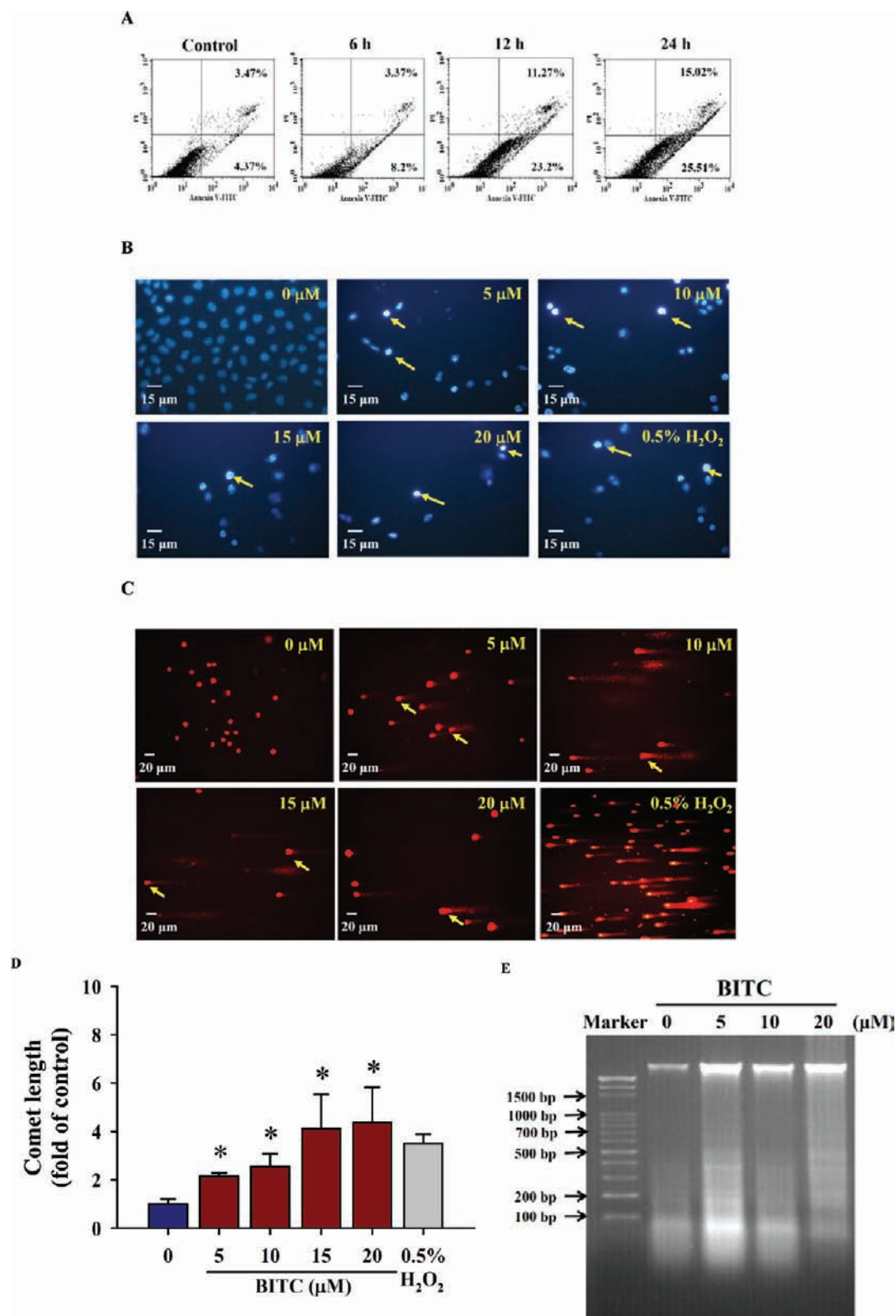


Figure 3. BITC induced DNA damage and apoptosis in A375.S2 cells. Cells were maintained and incubated with 10 μM BITC for various time periods following staining with annexin V (A) or with 0, 5, 10, 15, and 20 μM BITC for 24 h and then were isolated for the examination of apoptosis by DAPI staining (B), DNA damage using the comet assay (C), and quantification by CometScore software (D) or for the examination of apoptosis using DNA gel electrophoresis (E) and photographed under fluorescence microscopy as under Materials and Methods. The arrows show chromatin condensation and comet tail in BITC-treated cells when compared to the control group. Half-percent H_2O_2 was used as positive control. The data are shown in triplicates and exhibited similar results.

role of ROS production in BITC-induced apoptotic death in A375.S2 cells, cells were pretreated with a ROS scavenger

(NAC) and then exposed to BITC for 24 h. Results shown in Figure 7 indicated that NAC pretreatment in BITC-treated

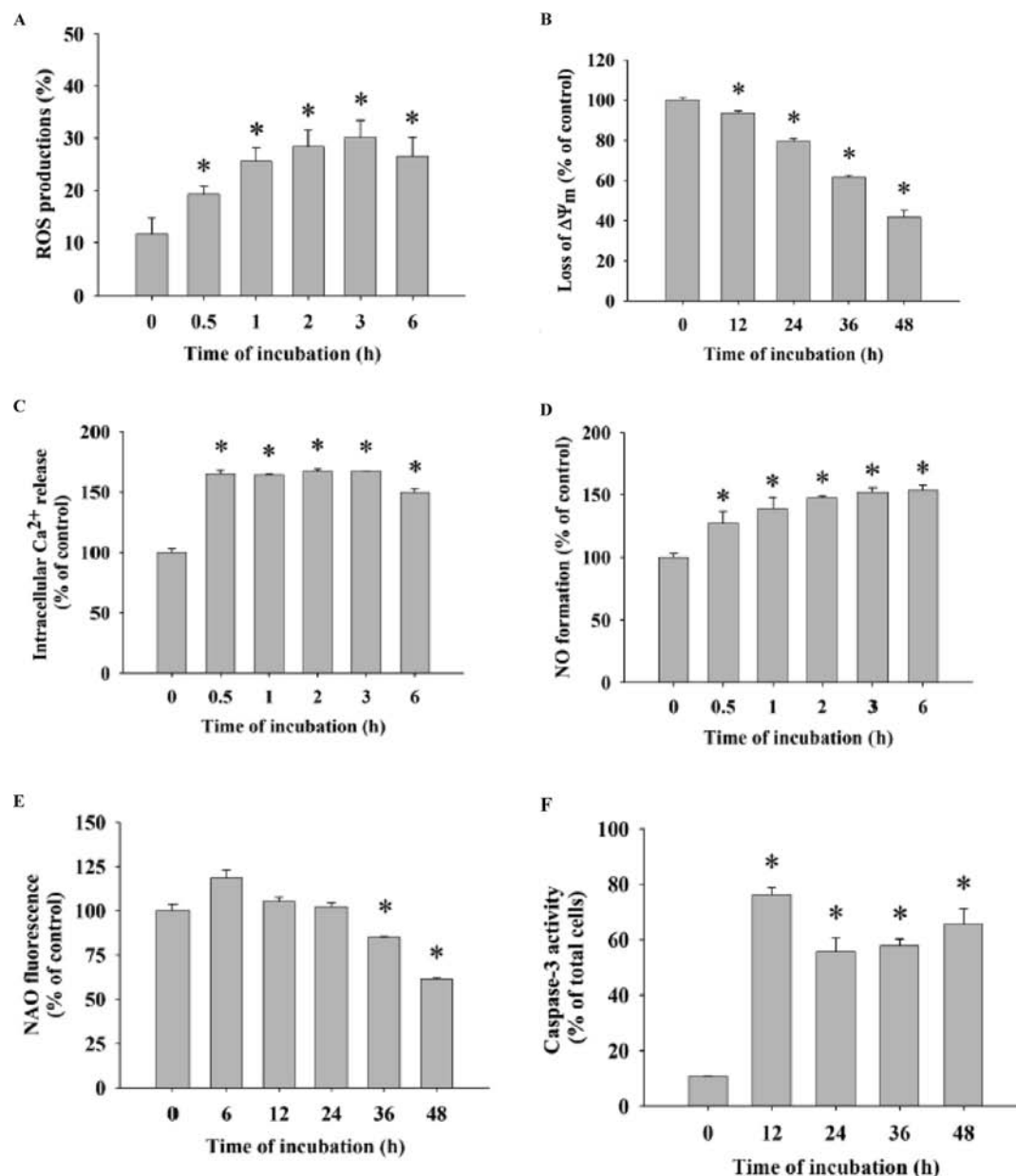


Figure 4. BITC affected the ROS production, the level of $\Delta\Psi_m$, intracellular Ca^{2+} release, NO and cardiolipin alterations, and caspase-3 activity in A375.S2 cells. Cells in 12-well plates were treated with or without 10 μ M BITC for various time periods, and then cells from each treatment were harvested and washed with PBS twice, resuspended in 500 μ L of H_2DCF -DA (10 μ M) for ROS, DiOC₆ (1 μ mol/L) for $\Delta\Psi_m$, Fluo-3/AM (2.5 μ g/mL) for Ca^{2+} release, DAF-FM (5 μ M) for NO, NAO (500 nM) for cardiolipin, and PhiPhiLux-G₁D₂ (10 μ M) for caspase-3. Cells then were incubated and were analyzed by flow cytometry as under Materials and Methods. The results are shown as the mean \pm SD ($n = 3$). An asterisk (*) indicates significant difference ($p < 0.05$) compared to control.

A375.S2 cells inhibited effects of BITC, resulting in a greater percentage of viable cells (Figure 7A), a reduction of cell debris morphology (Figure 7B), decreased chromatin condensation (Figure 7C) and ROS levels (Figure 7D), and loss of $\Delta\Psi_m$ (Figure 7E) in comparison to BITC-treated alone cells. On the basis of these observations, we confirmed that BITC-induced cell death in A375.S2 cells was mainly through a ROS-dependent apoptotic pathway.

DISCUSSION

BITC induces cell death via cell cycle arrest and induction of apoptosis in many types of human cancer cell lines, but there is no available information on BITC-induced apoptosis in human

melanoma cells. Here we show that BITC induced cytotoxic effects in human melanoma A375.S2 cells in vitro. Results from Figures 1 and 2 indicated that BITC induced cytotoxicity and reduced cell viability through induction of G₂/M phase arrest. Other investigators reported that cell cycle control represents a major regulatory mechanism for cell growth,³⁵ that anticancer agents can block the progression of cell cycle, and that such an approach should be considered for new cancer therapy in the future.^{36,37} Cell cycle progression is partly controlled by a family of protein kinase complexes in eukaryotic cells including cyclin-dependent kinases (CDKs) and their activating partners, the cyclins.³⁸

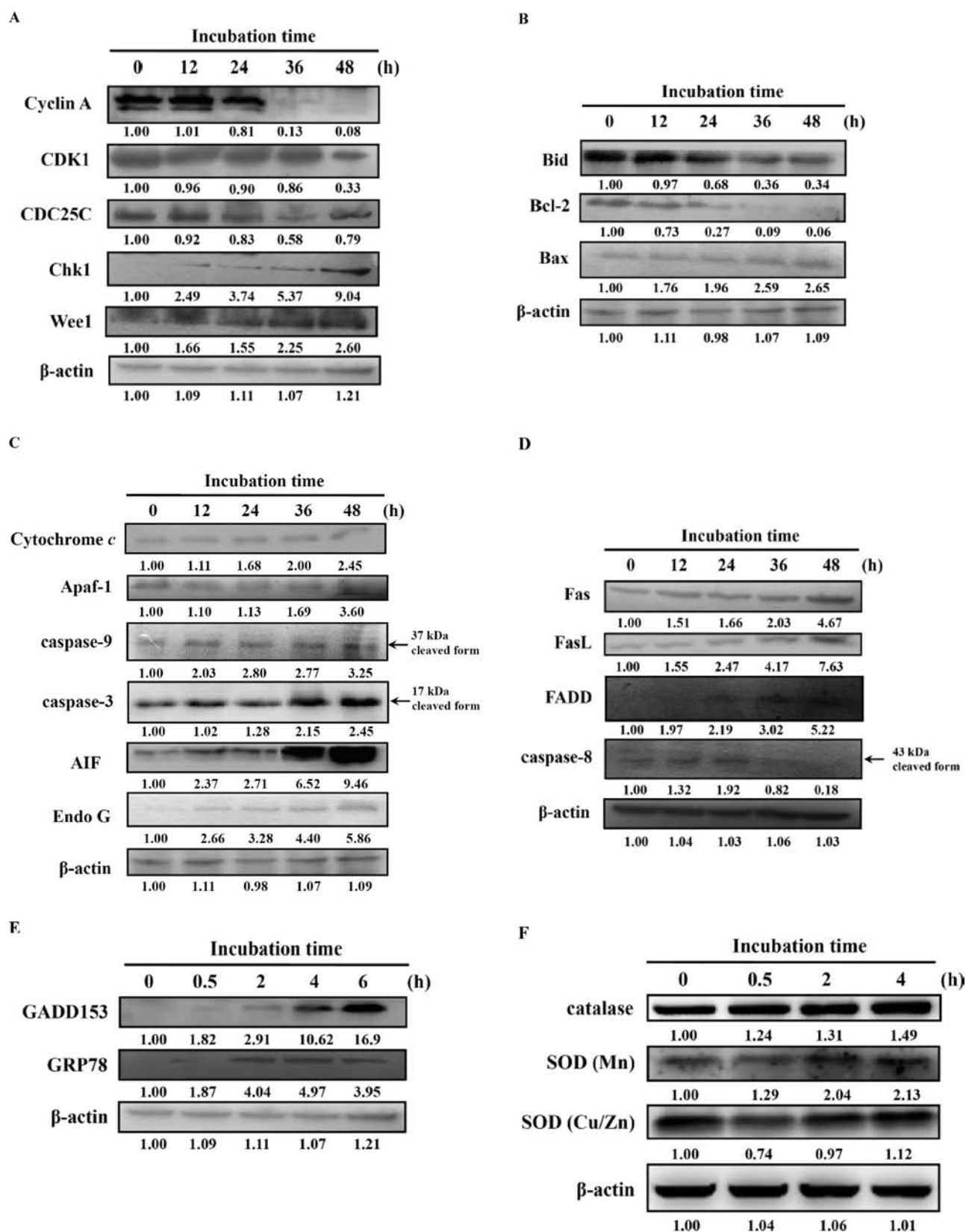


Figure 5. BITC altered the G₂/M arrest and apoptosis-associated proteins in A375.S2 cells. Cells (1×10^6 /well) seeded into 6-well plates were treated with 10 μ M BITC, incubated for 0, 12, 24, 36, and 48 h or for 0, 0.5, 2, 4 or 6 h, and then harvested for Western blotting to examine the protein levels of cyclin A, CDK1, CDC25C, Chk1, and Wee1 (A); Bid, Bcl-2, and Bax (B); cytochrome *c*, Apaf-1, caspase-9 and -3, AIF, and Endo G (C); Fas, FasL, FADD, and caspase-8 (D); GADD153 and GRP78 (E); and catalase, SOD(Cu/Zn), and SOD(Mn) (F) as described under Materials and Methods.

BITC treatment altered levels of proteins associated with the G₂/M phase. Results showed that the expression levels of cyclin

A, CDK1, and CDC25C (Figure 5A) were decreased, which is a critical complex regulating the G₂/M phase of the cell cycle in

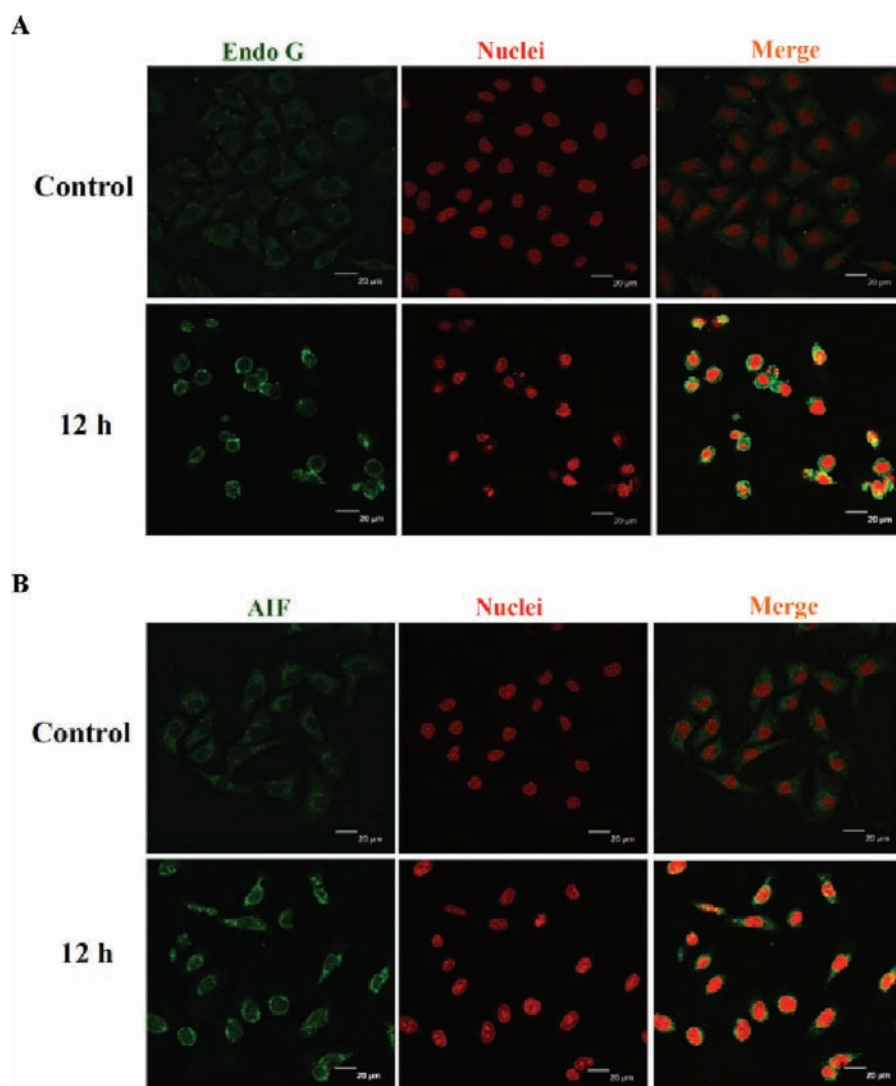


Figure 6. BITC translocated the AIF and Endo G expressions in A375.S2 cells. Cells at a density of 5×10^4 cells/well were placed on 4-well chamber slides, treated with $10 \mu\text{M}$ BITC for 12 h, and then fixed. The primary antibodies anti-Endo G (A) or anti-AIF (B) were used to stain the fixed cells overnight; the cells were then stained with secondary antibody (FITC-conjugated goat anti-mouse IgG at 1:100 dilution) (green fluorescence), followed by nuclei counterstaining with PI (red fluorescence). Photomicrographs were obtained using a Leica TCS SP2 confocal spectral microscope as described under Materials and Methods. Scale bar = $20 \mu\text{m}$.

A375.S2 cells. Furthermore, Chk1 and Wee1 (Figure 5A) protein levels associated with G_2/M phase arrest were increased in A375.S2 cells. On the basis of these observations, we propose that alterations in the levels of various cell cycle regulatory proteins were responsible for cell cycle arrest in BITC-induced death in A375.S2 cells. Cell cycle arrest may partially explain the induction of apoptosis and cytotoxic effects of BITC in A375.S2 cells.

In the present study, treatment with BITC caused sub- G_1 population augmentation, suggesting apoptosis was involved in BITC-induced A375.S2 cell death. Results from DNA gel electrophoresis showed DNA laddering formation (Figure 3D), and DAPI staining also revealed the appearance of apoptotic bodies (Figure 3B). These results are further evidence of BITC-induced apoptosis in A375.S2 cells. Kerr et al. have demonstrated that cells after exposure to an apoptosis inducer displayed activation of endonucleases and cleavage of DNA into fragments of approximately 180–200 base pairs.³⁹ Our results, shown in Figure 3E, indicated that BITC provoked DNA fragmentation in A375.S2 cells and are in agreement with the

earlier paper.³⁹ Our data also demonstrated that BITC promoted the levels of ROS, Ca^{2+} , NO, NAO, and caspase-3 activity in a time-dependent manner in A375.S2 cells but BITC decreased the levels of $\Delta\Psi_m$ (Figure 4).

In cells, the agent led to an increase in the levels of ROS, which can cause mitochondrial membrane depolarization,⁴⁰ and mitochondrial membrane depolarization is one of the earliest intracellular events of apoptosis.^{41,42} It was reported that the loss of $\Delta\Psi_m$ was mediated by the opening of the mitochondrial permeability transition pore,⁴³ which was regulated by Bcl-2 family proteins.⁴⁴ Results also showed that BITC increased levels of AIF and Endo G (Figure 6). BITC-induced ROS generation may involve the disruption of the mitochondrial membrane potential in A375.S2 cells. Bcl-2 family proteins (anti-apoptotic proteins such as Bcl-2 and Bcl-xl; pro-apoptotic proteins such as Bax and Bad)⁴⁵ are central regulators of apoptosis, and the interactions among these proteins would set the threshold for cell survival.⁴⁶ BITC treatment up-regulated pro-apoptotic members including Bax and Bid (Figure 5B), but the anti-apoptotic members such as Bcl-2 were significantly

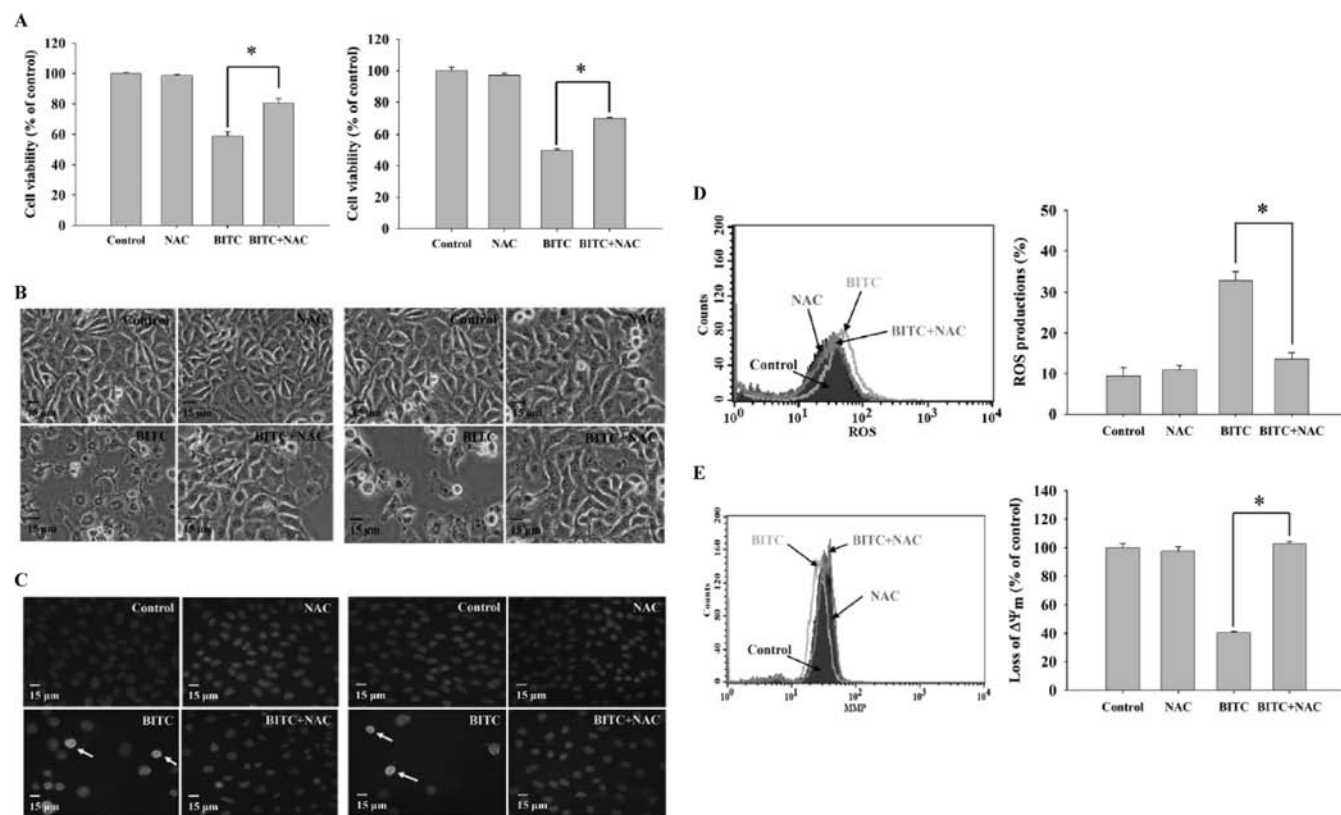


Figure 7. BITC affected the viable cell number, cell morphology, DAPI staining, ROS production, and level of $\Delta\Psi_m$ in A375.S2 cells. Cells (2×10^5 /well) placed in 12-well plates were pretreated with or without ROS scavenger (NAC) and exposed to $10 \mu\text{M}$ BITC for 24 h. Cells were harvested for measuring the percentage of viable cells (A), cell morphological changes (B), DAPI staining (C), level of ROS production (D), and level of $\Delta\Psi_m$ (E) as described under Materials and Methods. The arrows show chromatin condensation in apoptotic cells when compared to the control group. The results are shown as the mean \pm SD ($n = 3$), and * ($p < 0.05$) indicates significant difference when compared to untreated control.

down-regulated (Figure 5B). BITC altered the ratio of pro- and anti-apoptotic proteins in favor of apoptosis in A375.S2 cells.

BITC promoted cytochrome *c* release and caspase-3 activations (Figure 5C), which is in agreement with a high Bax/Bcl-2 ratio resulting in cytochrome *c* release.⁴⁷ Figure 4B indicated that BITC decreased the levels of $\Delta\Psi_m$ in A375.S2 cells. These effects could stimulate release of cytochrome *c* and reduce the mitochondrial membrane potential ($\Delta\Psi_m$) release.⁴⁸ Mitochondria may play an important role in regulating BITC-induced apoptotic death in A375.S2 cells. Figure 5F indicates that BITC promoted the expression of catalase and SOD (Mn) and SOD (Cu/Zn), which may led to ROS production. Furthermore, Figure 5E demonstrated that BITC promoted the expression of GRP78 and GADD153, and these observations indicated that BITC-induced apoptosis may be via ER stress in A375.S2 cells. In the present study, NAC (a ROS scavenger) was used to pretreat cells and then cells were incubated with BITC. NAC pretreatment caused a reduction in ROS levels (Figure 7A) and DNA condensation (Figure 7C) when compared to BITC treatment only and increased the percentage of viable cells (Figure 7D).

Overall, this study showed that BITC acted on regulatory factors (cyclin A, CDC25C, and Wee1) causing G_2/M phase arrest, halting cell cycle progression and inducing apoptosis through ROS production. This leads to ER stress and both mitochondrial dysfunction and Fas signal, leading to activation of caspase-3 and causing cell apoptosis in A375.S2 cells. A model depicting the actions of BITC is presented in Figure 8.

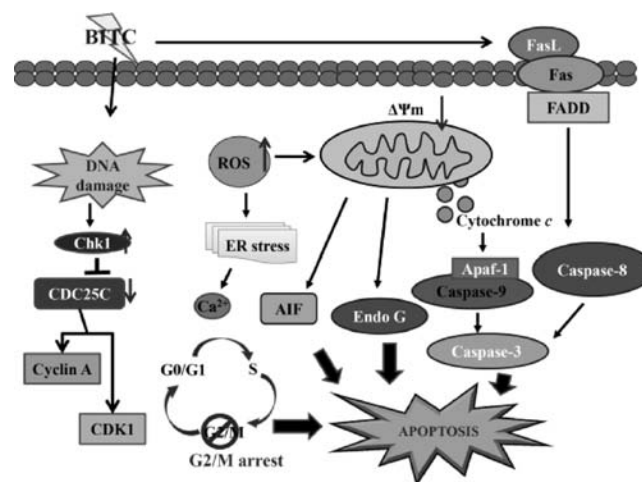


Figure 8. Possible signaling pathways for BITC-induced G_2/M phase arrest through cyclin A, CDC25C, Chk1, and Wee1 signaling and apoptosis via ROS-modulated ER stress, mitochondria- and death receptor-dependent multiple pathways in A375.S2 human melanoma cells.

BITC may have potential to be used in the treatment of melanoma.

■ AUTHOR INFORMATION

Corresponding Author

* (J.-G.C.) Postal address: Department of Biological Science and Technology, China Medical University, No. 91 Hsueh-Shih

Road, Taichung 404, Taiwan. Phone: +886 4 22053366, ext 2161. Fax: +886 4 22053764. E-mail: jgchung@mail.cmu.edu.tw. (C.-S.Y.) E-mail: csyu@mail.cmu.edu.tw..

Author Contributions

^{||}Both authors are equal contributors.

Funding

This research was supported by Grant CMU99-ASIA-22 from the China Medical University, Taichung, Taiwan.

ACKNOWLEDGMENTS

We thank Dr. Jen-Hung Yang, who kindly provided us with the HaCaT cell line for this study.

ABBREVIATIONS USED

$\Delta\Psi_m$, mitochondrial membrane potential; BITC, benzyl isothiocyanate; DAPI, 4',6-diamidino-2-phenylindole; DMSO, dimethyl sulfoxide; FBS, fetal bovine serum; NAC, N-acetyl-L-cysteine; PI, propidium iodide; ROS, reactive oxygen species.

REFERENCES

- (1) Sheridan, J. P.; Marsters, S. A.; Pitti, R. M.; Gurney, A.; Skubatch, M.; Baldwin, D.; Ramakrishnan, L.; Gray, C. L.; Baker, K.; Wood, W. I.; Goddard, A. D.; Godowski, P.; Ashkenazi, A. Control of TRAIL-induced apoptosis by a family of signaling and decoy receptors. *Science* **1997**, *277* (5327), 818–821.
- (2) Ashkenazi, A.; Dixit, V. M. Apoptosis control by death and decoy receptors. *Curr. Opin. Cell Biol.* **1999**, *11* (2), 255–260.
- (3) Kamachi, M.; Le, T. M.; Kim, S. J.; Geiger, M. E.; Anderson, P.; Utz, P. J. Human autoimmune sera as molecular probes for the identification of an autoantigen kinase signaling pathway. *J. Exp. Med.* **2002**, *196* (9), 1213–1225.
- (4) Porter, A. G.; Janicke, R. U. Emerging roles of caspase-3 in apoptosis. *Cell Death Differ.* **1999**, *6* (2), 99–104.
- (5) Tang, D.; Lahti, J. M.; Kidd, V. J. Caspase-8 activation and bid cleavage contribute to MCF7 cellular execution in a caspase-3-dependent manner during staurosporine-mediated apoptosis. *J. Biol. Chem.* **2000**, *275* (13), 9303–9307.
- (6) Caserta, T. M.; Smith, A. N.; Gultice, A. D.; Reedy, M. A.; Brown, T. L. Q-VD-OPH, a broad spectrum caspase inhibitor with potent antiapoptotic properties. *Apoptosis* **2003**, *8* (4), 345–352.
- (7) Khanbolooki, S.; Nawrocki, S. T.; Arumugam, T.; Andtbacka, R.; Pino, M. S.; Kurzrock, R.; Logsdon, C. D.; Abbruzzese, J. L.; McConkey, D. J. Nuclear factor-kappaB maintains TRAIL resistance in human pancreatic cancer cells. *Mol. Cancer Ther.* **2006**, *5* (9), 2251–2260.
- (8) Lam, T. K.; Gallicchio, L.; Lindsley, K.; Shiels, M.; Hammond, E.; Tao, X. G.; Chen, L.; Robinson, K. A.; Caulfield, L. E.; Herman, J. G.; Guallar, E.; Alberg, A. J. Cruciferous vegetable consumption and lung cancer risk: a systematic review. *Cancer Epidemiol. Biomarkers Prev.* **2009**, *18* (1), 184–195.
- (9) Verhoeven, D. T.; Goldbohm, R. A.; van Poppel, G.; Verhagen, H.; van den Brandt, P. A. Epidemiological studies on brassica vegetables and cancer risk. *Cancer Epidemiol. Biomarkers Prev.* **1996**, *5* (9), 733–748.
- (10) Cohen, J. H.; Kristal, A. R.; Stanford, J. L. Fruit and vegetable intakes and prostate cancer risk. *J. Natl. Cancer Inst.* **2000**, *92* (1), 61–68.
- (11) Conaway, C. C.; Yang, Y. M.; Chung, F. L. Isothiocyanates as cancer chemopreventive agents: their biological activities and metabolism in rodents and humans. *Curr. Drug Metab.* **2002**, *3* (3), 233–255.
- (12) Wu, X.; Zhou, Q. H.; Xu, K. Are isothiocyanates potential anti-cancer drugs? *Acta Pharmacol. Sin.* **2009**, *30* (5), 501–512.
- (13) Xiao, D.; Vogel, V.; Singh, S. V. Benzyl isothiocyanate-induced apoptosis in human breast cancer cells is initiated by reactive oxygen

species and regulated by Bax and Bak. *Mol. Cancer Ther.* **2006**, *5* (11), 2931–2945.

(14) Xiao, D.; Powolny, A. A.; Singh, S. V. Benzyl isothiocyanate targets mitochondrial respiratory chain to trigger reactive oxygen species-dependent apoptosis in human breast cancer cells. *J. Biol. Chem.* **2008**, *283* (44), 30151–30163.

(15) Tang, L.; Zhang, Y. Dietary isothiocyanates inhibit the growth of human bladder carcinoma cells. *J. Nutr.* **2004**, *134* (8), 2004–2010.

(16) Liu, K. C.; Huang, Y. T.; Wu, P. P.; Ji, B. C.; Yang, J. S.; Yang, J. L.; Chiu, T. H.; Chueh, F. S.; Chung, J. G. The roles of AIF and Endo G in the apoptotic effects of benzyl isothiocyanate on DU 145 human prostate cancer cells via the mitochondrial signaling pathway. *Int. J. Oncol.* **2011**, *38* (3), 787–796.

(17) Batra, S.; Sahu, R. P.; Kandala, P. K.; Srivastava, S. K. Benzyl isothiocyanate-mediated inhibition of histone deacetylase leads to NF-kappaB turnover in human pancreatic carcinoma cells. *Mol. Cancer Ther.* **2010**, *9* (6), 1596–1608.

(18) Kalkunte, S.; Swamy, N.; Dizon, D. S.; Brard, L. Benzyl isothiocyanate (BITC) induces apoptosis in ovarian cancer cells in vitro. *J. Exp. Ther. Oncol.* **2006**, *5* (4), 287–300.

(19) Tsou, M. F.; Peng, C. T.; Shih, M. C.; Yang, J. S.; Lu, C. C.; Chiang, J. H.; Wu, C. L.; Lin, J. P.; Lo, C.; Fan, M. J.; Chung, J. G. Benzyl isothiocyanate inhibits murine WEHI-3 leukemia cells in vitro and promotes phagocytosis in BALB/c mice in vivo. *Leuk. Res.* **2009**, *33* (11), 1505–1511.

(20) Mi, L.; Gan, N.; Chung, F. L. Isothiocyanates inhibit proteasome activity and proliferation of multiple myeloma cells. *Carcinogenesis* **2011**, *32* (2), 216–223.

(21) Wu, C. L.; Huang, A. C.; Yang, J. S.; Liao, C. L.; Lu, H. F.; Chou, S. T.; Ma, C. Y.; Hsia, T. C.; Ko, Y. C.; Chung, J. G. Benzyl isothiocyanate (BITC) and phenethyl isothiocyanate (PEITC)-mediated generation of reactive oxygen species causes cell cycle arrest and induces apoptosis via activation of caspase-3, mitochondria dysfunction and nitric oxide (NO) in human osteogenic sarcoma U-2 OS cells. *J. Orthop. Res.* **2011**, *29* (8), 1199–1209.

(22) Miyoshi, N.; Takabayashi, S.; Osawa, T.; Nakamura, Y. Benzyl isothiocyanate inhibits excessive superoxide generation in inflammatory leukocytes: implication for prevention against inflammation-related carcinogenesis. *Carcinogenesis* **2004**, *25* (4), 567–575.

(23) Lo, C.; Lai, T. Y.; Yang, J. H.; Yang, J. S.; Ma, Y. S.; Weng, S. W.; Chen, Y. Y.; Lin, J. G.; Chung, J. G. Gallic acid induces apoptosis in A375.S2 human melanoma cells through caspase-dependent and -independent pathways. *Int. J. Oncol.* **2010**, *37* (2), 377–385.

(24) Hsiao, Y. P.; Huang, H. L.; Lai, W. W.; Chung, J. G.; Yang, J. H. Antiproliferative effects of lactic acid via the induction of apoptosis and cell cycle arrest in a human keratinocyte cell line (HaCaT). *J. Dermatol. Sci.* **2009**, *54* (3), 175–184.

(25) Chiang, J. H.; Yang, J. S.; Ma, C. Y.; Yang, M. D.; Huang, H. Y.; Hsia, T. C.; Kuo, H. M.; Wu, P. P.; Lee, T. H.; Chung, J. G. Danthron, an anthraquinone derivative, induces DNA damage and caspase cascades-mediated apoptosis in SNU-1 human gastric cancer cells through mitochondrial permeability transition pores and Bax-triggered pathways. *Chem. Res. Toxicol.* **2011**, *24* (1), 20–29.

(26) Wu, S. H.; Hang, L. W.; Yang, J. S.; Chen, H. Y.; Lin, H. Y.; Chiang, J. H.; Lu, C. C.; Yang, J. L.; Lai, T. Y.; Ko, Y. C.; Chung, J. G. Curcumin induces apoptosis in human non-small cell lung cancer NCI-H460 cells through ER stress and caspase cascade- and mitochondria-dependent pathways. *Anticancer Res.* **2010**, *30* (6), 2125–2133.

(27) Lu, K. W.; Chen, J. C.; Lai, T. Y.; Yang, J. S.; Weng, S. W.; Ma, Y. S.; Lu, P. J.; Weng, J. R.; Chueh, F. S.; Wood, W. G.; Chung, J. G. Gypenosides inhibits migration and invasion of human oral cancer SAS cells through the inhibition of matrix metalloproteinase-2 -9 and urokinase-plasminogen by ERK1/2 and NF-kappa B signaling pathways. *Hum. Exp. Toxicol.* **2011**, *30* (5), 406–415.

(28) Kuo, T. C.; Yang, J. S.; Lin, M. W.; Hsu, S. C.; Lin, J. J.; Lin, H. J.; Hsia, T. C.; Liao, C. L.; Yang, M. D.; Fan, M. J.; Wood, W. G.; Chung, J. G. Emodin has cytotoxic and protective effects in rat C6

glioma cells: roles of Mdr1a and nuclear factor kappaB in cell survival. *J. Pharmacol. Exp. Ther.* **2009**, *330* (3), 736–744.

(29) Lu, C. C.; Yang, J. S.; Huang, A. C.; Hsia, T. C.; Chou, S. T.; Kuo, C. L.; Lu, H. F.; Lee, T. H.; Wood, W. G.; Chung, J. G. Chrysothanol induces necrosis through the production of ROS and alteration of ATP levels in J5 human liver cancer cells. *Mol. Nutr. Food Res.* **2010**, *54* (7), 967–976.

(30) Chung, J. G.; Yang, J. S.; Huang, L. J.; Lee, F. Y.; Teng, C. M.; Tsai, S. C.; Lin, K. L.; Wang, S. F.; Kuo, S. C. Proteomic approach to studying the cytotoxicity of YC-1 on U937 leukemia cells and antileukemia activity in orthotopic model of leukemia mice. *Proteomics* **2007**, *7* (18), 3305–3317.

(31) Chen, J. C.; Lu, K. W.; Tsai, M. L.; Hsu, S. C.; Kuo, C. L.; Yang, J. S.; Hsia, T. C.; Yu, C. S.; Chou, S. T.; Kao, M. C.; Chung, J. G.; Wood, W. G. Gypenosides induced G0/G1 arrest via Chk2 and apoptosis through endoplasmic reticulum stress and mitochondria-dependent pathways in human tongue cancer SCC-4 cells. *Oral Oncol.* **2009**, *45* (3), 273–283.

(32) Fusenig, N. E.; Boukamp, P. Multiple stages and genetic alterations in immortalization, malignant transformation, and tumor progression of human skin keratinocytes. *Mol. Carcinogenesis* **1998**, *23* (3), 144–158.

(33) Altenburger, R.; Kissel, T. The human keratinocyte cell line HaCaT: an in vitro cell culture model for keratinocyte testosterone metabolism. *Pharm. Res.* **1999**, *16* (5), 766–771.

(34) Bonnekoh, B.; Farkas, B.; Geisel, J.; Mahrle, G. Lactate dehydrogenase release as an indicator of dithranol-induced membrane injury in cultured human keratinocytes. A time profile study. *Arch. Dermatol. Res.* **1990**, *282* (5), 325–329.

(35) Jeong, H. W.; Han, D. C.; Son, K. H.; Han, M. Y.; Lim, J. S.; Ha, J. H.; Lee, C. W.; Kim, H. M.; Kim, H. C.; Kwon, B. M. Antitumor effect of the cinnamaldehyde derivative CB403 through the arrest of cell cycle progression in the G2/M phase. *Biochem. Pharmacol.* **2003**, *65* (8), 1343–1350.

(36) Buolamwini, J. K. Cell cycle molecular targets in novel anticancer drug discovery. *Curr. Pharm. Des.* **2000**, *6* (4), 379–392.

(37) McDonald, E. R.; El-Deiry, W. S. Cell cycle control as a basis for cancer drug development (review). *Int. J. Oncol.* **2000**, *16* (5), 871–886.

(38) Malumbres, M.; Barbacid, M. Mammalian cyclin-dependent kinases. *Trends Biochem. Sci.* **2005**, *30* (11), 630–641.

(39) Kerr, J. F.; Winterford, C. M.; Harmon, B. V. Apoptosis. Its significance in cancer and cancer therapy. *Cancer* **1994**, *73* (8), 2013–2026.

(40) Rogalska, A.; Koceva-Chyla, A.; Jozwiak, Z. Aclarubicin-induced ROS generation and collapse of mitochondrial membrane potential in human cancer cell lines. *Chem.–Biol. Interact.* **2008**, *176* (1), 58–70.

(41) Desagher, S.; Martinou, J. C. Mitochondria as the central control point of apoptosis. *Trends Cell Biol.* **2000**, *10* (9), 369–377.

(42) Han, J.; Goldstein, L. A.; Gastman, B. R.; Rabinowich, H. Interrelated roles for Mcl-1 and BIM in regulation of TRAIL-mediated mitochondrial apoptosis. *J. Biol. Chem.* **2006**, *281* (15), 10153–10163.

(43) Zoratti, M.; Szabo, I. The mitochondrial permeability transition. *Biochim. Biophys. Acta* **1995**, *1241* (2), 139–176.

(44) Tsujimoto, Y. Cell death regulation by the Bcl-2 protein family in the mitochondria. *J. Cell Physiol.* **2003**, *195* (2), 158–167.

(45) Burlacu, A. Regulation of apoptosis by Bcl-2 family proteins. *J. Cell Mol. Med.* **2003**, *7* (3), 249–257.

(46) Borner, C. The Bcl-2 protein family: sensors and checkpoints for life-or-death decisions. *Mol. Immunol.* **2003**, *39* (11), 615–647.

(47) Yang, J.; Liu, X.; Bhalla, K.; Kim, C. N.; Ibrado, A. M.; Cai, J.; Peng, T. I.; Jones, D. P.; Wang, X. Prevention of apoptosis by Bcl-2: release of cytochrome c from mitochondria blocked. *Science* **1997**, *275* (5303), 1129–1132.

(48) Bustamante, J.; Caldas Lopes, E.; Garcia, M.; Di Libero, E.; Alvarez, E.; Hajos, S. E. Disruption of mitochondrial membrane potential during apoptosis induced by PSC 833 and CsA in multidrug-resistant lymphoid leukemia. *Toxicol. Appl. Pharmacol.* **2004**, *199* (1), 44–51.